Electrochimica Acta 55 (2010) 5230–5238

Contents lists available at ScienceDirect

Electrochimica Acta

journal homepage: www.elsevier.com/locate/electacta

Mathematical modeling of diffusion and kinetics in amperometric immobilized enzyme electrodes

S. Loghambal, L. Rajendran*

Department of Mathematics, Madura College, Madurai 625011, Tamil Nadu, India

ARTICLE INFO

Article history:
Received 29 January 2010
Received in revised form 9 April 2010
Accepted 9 April 2010
Available online 18 April 2010

Keywords:
Amperometric electrodes
Redox enzyme
Diffusion-reaction equations
Michaelis–Menten kinetics
Homotopy perturbation method

ABSTRACT

An analysis of the diffusion and kinetics in amperometric immobilized enzyme electrodes is presented for reactions of the enzyme and substrate. This analysis contains a non-linear term related to Michaelis–Menten kinetics. In this paper, we obtain approximate analytical solutions for the non-linear equations that describe diffusion and the reaction within the film by employing the homotopy perturbation method (HPM). The obtained analytical results are compared with the available limiting case results and found to be in satisfactory agreement.

1. Introduction

Recently, there has been much interest in the development of amperometric enzyme electrodes [1,2]. Rahmathunissa and Rajendran [3] obtained the analytical solutions for substrate concentration and transient current for both steady-state and non-steady-state amperometric polymer-modified electrodes using Danckwerts' relation. Andrieux et al. [4] and Albery and Hillman [5] analyzed the kinetics of reactions at polymer-modified electrodes. During these reactions, species from the solution react with a mediator that was bound in a film at the electrode surface. The approximate analytical solutions can be obtained for limiting cases by linearizing the non-linear term [6]. In the case of an immobilized enzyme, the problem is further complicated by the non-linear enzyme kinetics. For the enzyme kinetics problem, approximate analytical solutions have been developed by Blaedel et al. [7], Kulys et al. [8] and Bartlett and Whitaker [9] for the only the limiting cases (saturated and unsaturated). The applications of numerical and approximate analytical methods can be seen in Bartlett and Pratt [10]. The numerical simulation can be found in Bartlett and coworkers [11]. Senthamarai and Rajendran derived the approximate analytical expressions for the substrate, mediator concentrations and current for the non-linear Michaelis–Menten kinetic scheme in a system of coupled non-linear reaction-diffusion processes at conducting polymer-modified ultramicroelectrodes [12] using the variational iteration method. In this paper, we present the approximate analytical expressions for the concentrations of the mediator and substrate. These concentrations were determined using homotopy perturbation method (HPM) [13,14]. The current was determined corresponding to all possible values of the parameters a_ε, κ, γ, η, and μ. These parameters are explained below in Eq. (10).

2. Mathematical formulation of the problem and analysis

2.1. Mathematical formulation

Fig. 1 shows the general kinetic scheme for an enzyme-membrane/electrode. A and B are the oxidized and reduced forms of the mediator, respectively. E_1 and E_2 are the oxidized and reduced forms of the enzyme, respectively. S and P are the substrate and the product of the enzymatic reaction, respectively. Diffusion of mediator A and substrate S occurs within the film with diffusion coefficients D_A and D_S, respectively. Partition of the substrate between the film and the bulk solution is described by the partition coefficient K_S. The mediator partition is described by K_A. The reactions that occur within the film (Fig. 1) in the kinetic scheme can be written as follows:

$$A + E_2 \xrightarrow{k_A} B + E_1 \tag{1}$$

$$E_1 + S \xrightarrow{k_E} E_2 + P, \tag{2}$$

and the reaction at the electrode is $B \rightarrow A$.

* Corresponding author. Tel.: +91 0452 2673354; fax: +91 0452 2675238.
E-mail address: raj_sms@rediffmail.com (L. Rajendran).

0013-4686/$ – see front matter © 2010 Elsevier Ltd. All rights reserved.
doi:10.1016/j.electacta.2010.04.050

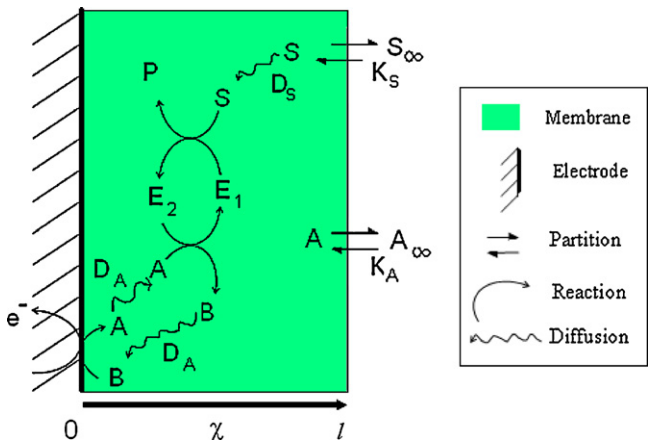

Fig. 1. Schematic representation of a typical enzyme-membrane|electrode showing the processes considered in the model. The homogenous enzyme kinetics that occurs throughout the film is described by Eqs. (1)–(3).

Here, k_E and k_A are second-order rate constants that describe the reaction between the enzyme and the substrate and between the enzyme and the mediator, respectively. According to Michaelis–Menten kinetics, the following is true:

$$k_E = \frac{k_{cat}}{K_M + [S]}, \tag{3}$$

where k_{cat} denotes the catalytic rate constant, and K_M denotes the Michaelis–Menten constant. The homogenous enzyme kinetics described by Eqs. (1)–(3) occurs throughout the film from $x = 0$ to $x = l$, where l is the thickness of the membrane. We consider a situation in which the mediator is entrapped within the film. This situation does not include a separate soluble redox mediator that is re-oxidized on a conducting entrapment matrix. Here, the rate constants for a heterogeneous reaction on the supporting matrix must be considered. The differential equations that quantify the diffusion and reaction within the film may be written as follows [6]:

$$\frac{\partial[S]}{\partial t} = D_S \frac{\partial^2[S]}{\partial x^2} - \frac{k_{cat}\,[E_1][S]}{K_M + [S]} \tag{4}$$

$$\frac{\partial[A]}{\partial t} = D_A \frac{\partial^2[A]}{\partial x^2} - k_A\,[E_2][A] \tag{5}$$

$$\frac{\partial[E_1]}{\partial t} = k_A[A][E_2] - \frac{k_{cat}[E_1][S]}{K_M + [S]} \tag{6}$$

Assuming that the enzyme is bound within the film, is not free to diffuse and is in the steady-state $d[E_1]/dt = 0$, Eq. (6) leads to the following:

$$[E_2] = \frac{k_{cat}[E_\Sigma][S]}{k_A[A](K_M + [S]) + k_{cat}[S]}, \tag{7}$$

where $[E_\Sigma] = [E_1] + [E_2]$ denotes the total concentration of the immobilized enzyme. Then, in the steady-state, Eqs. (4) and (5) are reduced to the following:

$$D_A \frac{d^2[A]}{dx^2} = \frac{k_A\,k_{cat}[A][S][E_\Sigma]}{k_A[A](K_M + [S]) + k_{cat}[S]} \tag{8}$$

$$D_S \frac{d^2[S]}{dx^2} = \frac{k_A\,k_{cat}[A][S][E_\Sigma]}{k_A[A](K_M + [S]) + k_{cat}[S]}. \tag{9}$$

Eqs. (8) and (9) are solved for the following boundary conditions:

$$x = l, \quad [S] = [S]_\infty K_S \tag{9a}$$

$$x = 0, \quad \frac{d[S]}{dx} = 0 \tag{9b}$$

$$x = 0, \quad [A] = [A]_\varepsilon \tag{9c}$$

and

$$x = l, \quad \frac{d[A]}{dx} = 0 \tag{9d}$$

We make the non-linear differential Eqs. (8) and (9) dimensionless by defining the following parameters:

$$a = \frac{[A]}{K_A[B_\Sigma]_\infty}, \quad s = \frac{[S]}{K_S[S]_\infty}, \quad \chi = \frac{x}{l}, \quad \kappa = l\left(\frac{k_A[E_\Sigma]}{D_A}\right)^{1/2},$$
$$\eta = \frac{D_S\,k_A\,K_M}{D_A\,k_{cat}}, \quad \gamma = \frac{k_A\,K_A[B_\Sigma]_\infty\,K_M}{k_{cat}\,K_S[S]_\infty}, \quad \mu = \frac{K_S[S]_\infty}{K_M} \tag{10}$$

where a is the dimensionless concentration of the mediator and s is the dimensionless concentration of the substrate. χ is the normalized distance from the electrode/membrane interface. κ describes the equilibrium constant between the diffusion of B within the film and its reaction with the enzyme. η denotes the relative amount of depletion of the substrate and oxidized mediator within the film. The parameter γ represents the equilibrium constant between the two forms of the enzyme. The ratio of the substrate concentration within the film to the Michaelis constant is described by μ. The subscript ∞ denotes the concentration in the bulk solution. a and s are normalized with respect to the total concentrations $K_A[B_\Sigma]$ and $K_S[S]_\infty$ of the two species within the film, where $[B_\Sigma] = [A] + [B]$, $K_A[B_\Sigma]_\infty = [B_\Sigma]$, and $K_S[S]_\infty = [S] + [P]$. When $\kappa \ll 1$, B can diffuse across the film before it reacts with the enzyme. For $\eta \ll 1$, consumption of the substrate is greater than mediator reduction, and for $\eta \gg 1$, the mediator reduction is greater than consumption of the substrate. For $\gamma \ll 1$, all of the enzymes are in the E_2 form. For unsaturated Michaelis–Menten kinetics, $\mu \ll 1$. For saturated kinetics, $\mu \gg 1$. Eqs. (8) and (9) reduce to the following dimensionless forms:

$$\frac{d^2s}{d\chi^2} = \frac{\gamma\,\eta^{-1}\,\kappa^2\,as}{\gamma\,a(1 + \mu s) + s} \tag{11}$$

$$\frac{d^2a}{d\chi^2} = \frac{\kappa^2\,as}{\gamma\,a(1 + \mu\,s) + s} \tag{12}$$

The dimensionless boundary conditions for Eqs. (11) and (12) are as follows:

$$\chi = 1, \quad s = 1 \tag{12a}$$

$$\chi = 0, \quad \frac{ds}{dx} = 0 \tag{12b}$$

$$\chi = 0, \quad a = a_\varepsilon \tag{12c}$$

and

$$\chi = 1, \quad \frac{da}{dx} = 0. \tag{12d}$$

The parameter ε is the dimensionless potential, which can be defined as:

$$\varepsilon = \frac{(E - E^0)nF}{RT} \tag{13}$$

where E is the potential of an electrode, E^0 is the standard potential of an electrode, n is the number of electrons, F is the Faraday constant, R is the universal gas constant and T is the absolute temperature. Combining the Nernst equation $E = E^0 + (RT/nF)\,\ln([A]_0/[B]_0)$ and Eq. (13) gives the dimensionless oxidized mediator concentration a_ε at the electrode surface:

$$a_\varepsilon = \frac{1}{1 + \exp(-\varepsilon)} \tag{14}$$

Here $[A]_0$ and $[B]_0$ denote the concentration of the two forms of the mediator at the electrode surface. Eq. (14) gives the boundary condition for a at the electrode surface. The dimensionless flux

Table 1
Various expressions of the mediator concentration a and the substrate concentration s (Pratt et al. [6]).

Limiting cases	Pratt's work		Fig no.		
	a	s	a		s	
Mediator-limited kinetics $\frac{a}{s} < \frac{1}{\gamma(1+\mu s)}$	$a = a_\varepsilon\,[\cosh(\chi\kappa) - \tanh(\kappa)\,\sinh(\chi\kappa)]$ (23)	–	Fig. 2 ($\kappa < 1$) (Eqs. (17) and (23)) $\kappa = 0.1$, $\gamma = 0.001$, $\eta = 10$, $\mu = 0.001$, $a_\varepsilon = 1$ Fig. 2 ($\kappa > 1$) (Eqs. (17) and (23)) $\kappa = 5$, $\gamma = 0.001$, $\eta = 10$, $\mu = 0.01$, $a_\varepsilon = 1$	$\kappa = 10$, $\gamma = 0.001$, $\eta = 10$, $\mu = 0.001$, $a_\varepsilon = 1$	Fig. 3 ($\kappa < 1$) (Eq. (20)) $\kappa = 0.1$, $\gamma = 0.01$, $\eta = 0.1$, $\mu = 0.1$, $a_\varepsilon = 1$ Fig. 3 ($\kappa > 1$) (Eq. (20)) $\kappa = 10$, $\gamma = 0.01$, $\eta = 0.1$, $\mu = 0.1$, $a_\varepsilon = 1$	
Substrate-limited kinetics $\frac{a}{s} > \frac{1}{\gamma(1+\mu s)}$	–	$s = \frac{\cosh(\chi\kappa/\eta^{1/2})}{\cosh(\kappa/\eta^{1/2})}$ (24)	Fig. 5 ($\kappa < 1$) (Eq. (17)) $\kappa = 0.1$, $\gamma = 2$, $\eta = 4$, $\mu = 0.001$, $a_\varepsilon = 1$ Fig. 5 ($\kappa > 1$) (Eq. (17)) $\kappa = 5$, $\gamma = 2$, $\eta = 4$, $\mu = 0.001$, $a_\varepsilon = 1$		Fig. 6 ($\kappa < 1$) $\kappa = 0.1$, $\gamma = 100$, $\eta = 10^5$, $\mu = 0.01$, $a_\varepsilon = 0.01$ Fig. 6 ($\kappa > 1$) (Eqs. (20) and (24)) $\kappa = 5$, $\gamma = 100$, $\eta = 10^5$, $\mu = 0.01$, $a_\varepsilon = 0.01$	$\kappa = 10$, $\gamma = 100$, $\eta = 10^5$, $\mu = 0.01$, $a_\varepsilon = 0.01$

Table 2
Expression for the concentration of the mediator in the thin film approximation (Pratt et al. [6]).

Conditions	Pratt's work for thin film approximation	Fig no.
$\frac{\kappa^2}{\eta} < 1$ and $s = 1$	$a = [a_\varepsilon + \gamma(1+\mu)]\left\{\cosh\left[\frac{\chi\kappa}{1+\gamma(1+\mu)}\right] - \tanh\left[\frac{\kappa}{1+\gamma(1+\mu)}\right]\sinh\left[\frac{\chi\kappa}{1+\gamma(1+\mu)}\right]\right\} - \gamma(1+\mu)$ (25)	Fig. 8 ($\kappa<1$) (Eqs. (19) and (25)) $\kappa=0.1, \gamma=10^{-5}, \mu=0.1, a_\varepsilon=1$ Fig. 8 ($\kappa>1$) (Eqs. (19) and (25)) $\kappa=10, \gamma=10^{-5}, \mu=0.1, a_\varepsilon=1$ $\kappa=5, \gamma=10^{-5}, \mu=0.1, a_\varepsilon=1$

of substrate (J_S) consumed at the electrode is considered as the following:

$$J_S = \frac{lj_S}{D_A[B_\Sigma]_\infty K_A} = \frac{\eta}{\gamma}\left(\frac{ds}{d\chi}\right)_{\chi=1} = \left(\frac{da}{d\chi}\right)_{\chi=1} - \left(\frac{da}{d\chi}\right)_{\chi=0}, \quad (15)$$

and that of the mediator (J_{obs}) measured at the electrode is as follows:

$$J_{obs} = \frac{lj_{obs}}{D_A[B_\Sigma]_\infty K_A} = -\left(\frac{da}{d\chi}\right)_{\chi=0}. \quad (16)$$

With respect to the boundary condition, the flux of the substrate reacting within the film is equal to the observed flux: $J_{obs} = J_S$.

2.2. Solution of boundary value problem using the HPM

Recently, many authors have applied the HPM to various problems and demonstrated the efficiency of the HPM for handling non-linear structures and solving various physics and engineering problems [15–18]. This method is a combination of homotopy in topology and classic perturbation techniques. Ji-Huan He used the HPM to solve the Lighthill equation [19], the Duffing equation [20] and the Blasius equation [21]. The idea has been used to solve non-linear boundary value problems [22], integral equations [23–25], Klein–Gordon and Sine–Gordon equations [26], Emden–Flower type equations [27] and many other problems. This wide variety of applications shows the power of the HPM to solve functional equations. The HPM is unique in its applicability, accuracy and efficiency. The HPM [28] uses the imbedding parameter p as a small parameter, and only a few iterations are needed to search for an asymptotic solution. Using this method (see Appendix B), we can obtain the following solution to Eq. (11):

$$a = W_1 \cosh\kappa[\cosh(2\kappa(1-\chi)) - 3] + \cosh(\kappa(1-\chi))[W_2 + W_1(3 - \cosh 2\kappa)] - W_3(W_4 + W_5 + W_6)(2\chi - \chi^2) \quad (17)$$

where

$$W_1 = \frac{\gamma a_\varepsilon^2(1+\mu)}{6\cosh^3\kappa}, \quad W_2 = \frac{a_\varepsilon}{\cosh\kappa}, \quad W_3 = \frac{(\kappa\gamma)^2 a_\varepsilon^3}{2(e^{2\kappa}+1)\eta},$$
$$W_4 = 1 - 2e^\kappa + \kappa + \eta, \quad W_5 = (1+e^{2\kappa})\eta\mu(2+\mu),$$
$$W_6 = e^{2\kappa}(1-\kappa+\eta) \quad (18)$$

Eq. (17) represents the analytical expression of the mediator concentration for all values of the parameters κ, γ, η, μ, and a_ε. Eq. (17) satisfies the boundary conditions at $\chi=0$, $a=a_\varepsilon$ and at $\chi=1$, $da/d\chi=0$. In the thin film approximation case in which $\kappa^2/\eta<1$ and the substrate can diffuse much further than the thickness of the film before it reacts with the enzyme, the result is $s\approx1$. Therefore, the expression of the mediator concentration becomes the following:

$$a = W_1 \cosh\kappa[\cosh(2\kappa(1-\chi)) - 3] + \cosh(\kappa(1-\chi))[W_2 + W_1(3 - \cosh 2\kappa)] \quad (19)$$

The solution to Eq. (12) is as follows:

$$s = 1 - W_8(1 + \kappa\sinh\kappa) + W_7(1 + 2\kappa\sinh 2\kappa) + 6W_7\kappa^2 + [W_8\kappa\sinh\kappa - 2W_7\kappa\sinh 2\kappa]\chi - 6\kappa^2 W_7\chi^2 + W_8\cosh(\kappa(1-\chi)) - W_7\cosh(2\kappa(1-\chi)) \quad (20)$$

where

$$W_7 = \frac{W_1\gamma\cosh\kappa}{2\eta}, \quad W_8 = \frac{\gamma}{\eta}[W_1(3 - \cosh 2\kappa) + W_2] \quad (21)$$

Eq. (20) represents the analytical expression of the substrate concentration for all values of the parameters κ, γ, η, μ, and a_ε. Eq. (20) satisfies the boundary conditions at $\chi=1$, $s=1$ and $\chi=0$, $ds/d\chi=0$. From Eqs. (15) and (19), we can obtain the dimensionless flux, which is as follows:

$$J_S = J_{obs} = \frac{\eta}{\gamma}(W_8\sinh\kappa - 2W_7\sinh 2\kappa - 12W_7\kappa) \quad (22)$$

Table 3
Various expressions of the dimensionless current (Pratt et al. [6]).

Limiting cases	Pratt's work Flux $J_{obs} = J_s$	Fig no.
Mediator-limited kinetics $a/s < 1/\gamma(1+\mu s)$	$J_{obs} = \kappa a_\varepsilon \tanh(\kappa)$, $J_{obs} = \kappa^2 a_\varepsilon$, for $\kappa<1$, $J_{obs} = \kappa a_\varepsilon$, for $\kappa>1$ (26)	Fig. 9 (Eqs. (22) and (26)) $\kappa=0.01, \gamma=0.001, \eta=0.1, \mu=0.01$
Substrate-limited kinetics $a/s > 1/\gamma(1+\mu s)$	$J_S = \frac{\eta^{1/2}\kappa}{\gamma}\tanh\left[\frac{\kappa}{\eta^{1/2}(1+\mu)}\right]$, $J_{obs} = \frac{\kappa^2}{\gamma(1+\mu)}$, for $\kappa < \eta^{1/2}(1+\mu)$, $J_{obs} = \frac{\eta^{1/2}\kappa}{\gamma}$, for $\kappa > \eta^{1/2}(1+\mu)$ (27)	Fig. 10 (Eqs. (22 and 27)) $\gamma=10, \eta=0.01, \mu=0.01, a_\varepsilon=0.01$
Thin film approximation $\frac{\kappa^2}{\eta} < 1$	$J_{obs} = \frac{\kappa[a_\varepsilon + \gamma(1+\mu)]}{1+\gamma(1+\mu)}\tanh\left[\frac{\kappa}{1+\gamma(1+\mu)}\right]$ (28)	Fig. 11 (Eqs. (22 and 28)) $\kappa=0.01, \gamma=0.01, \eta=0.1, a_\varepsilon=0.01$

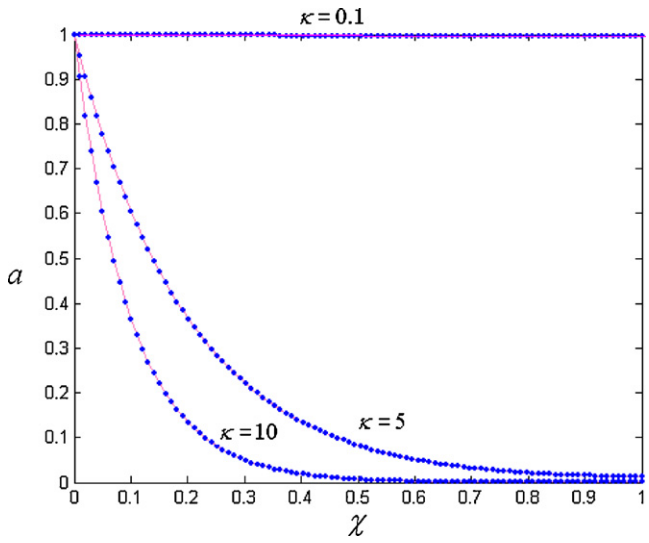

Fig. 2. Plot of the two-dimensional comparative case diagram of the mediator concentration a versus the normalized distance χ when $\gamma a < s/(1+\mu s)$ for $\gamma = 0.001$, $\eta = 10$, $\mu = 0.001$ and $a_\varepsilon = 1$ and various values of κ. — is plotted according to Eq. (17), and ··· is plotted according to Eq. (23).

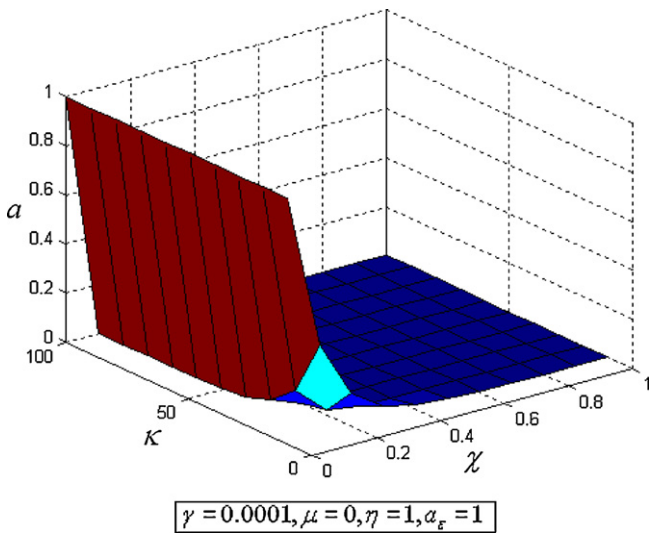

Fig. 4. The normalized three-dimensional mediator concentration profiles of a calculated using Eq. (17) for κ in the range of 0–100.

where W_7 and W_8 are given by Eq. (21). Eq. (17) and Eq. (20) are the closed forms of the approximate analytical expressions of the concentrations of the mediator and substrate for all values of the parameters κ, γ, η, μ, and a_ε. Eq. (22) is the new approximate expression of the flux.

3. Results and discussion

Pratt and co-worker [6] derived the approximate analytical solutions of the mediator and the substrate concentrations and the current for different limiting cases. Various analytical expressions for the concentration of the mediator and substrate for $a/s < 1/\gamma(1+\mu s)$ and $a/s > 1/\gamma(1+\mu s)$ are given in Table 1. The analytical expression for the thin film approximation is given in Table 2. The analytical expressions for the dimensionless current derived by Pratt and co-worker [6] for various limiting cases are given in Table 3.

3.1. Comparison with the work of Pratt and co-worker [6]

3.1.1. Mediator-limited kinetics ($a/s < 1/\gamma(1+\mu s)$)

In this case, the mediator–enzyme reaction is the rate-determining step. Figs. 2 and 3 represent the concentration profiles of the mediator and the substrate for various values of the parameters κ, γ, η, μ, and a_ε, respectively. The concentration of the mediator a is closer to unity when the values of all of the parameters are less than 0.4. The concentration of the substrate s is equal to unity when the values of all of the parameters are less than 1. When $\kappa > 1$, the concentration of the mediator a decreases quickly when $\chi \leq 0.5$, and a reaches the steady-state value zero when $\chi \geq 0.5$ (Fig. 2). However, the concentration of the substrate increases gradually (Fig. 3). Fig. 4 shows the normalized mediator concentration profiles of a for various values of κ and χ. This data confirm that the concentration profiles of the mediator a decrease when κ increases for all values of distance χ.

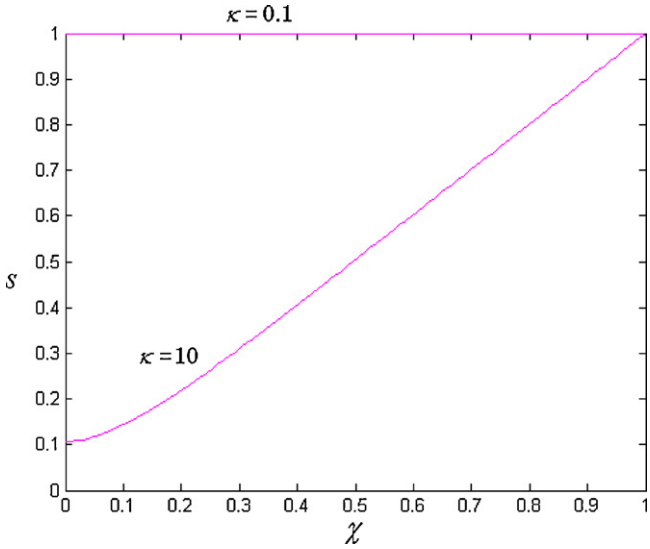

Fig. 3. Plot of the two-dimensional diagram of the substrate concentration s versus the normalized distance χ when $\gamma a < s/(1+\mu s)$ for $\gamma = 0.01$, $\eta = 0.1$, $\mu = 0.1$ and $a_\varepsilon = 1$ and various values of κ. — is plotted according to Eq. (20).

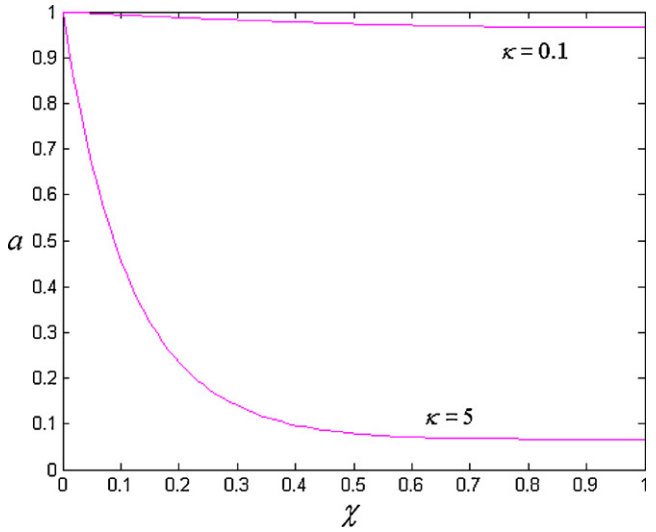

Fig. 5. Plot of the two-dimensional diagram of the mediator concentration a versus the normalized distance χ when $\gamma a > s/(1+\mu s)$ for $\gamma = 2$, $\eta = 4$, $\mu = 0.001$ and $a_\varepsilon = 1$ and various values of κ. — is plotted according to Eq. (17).

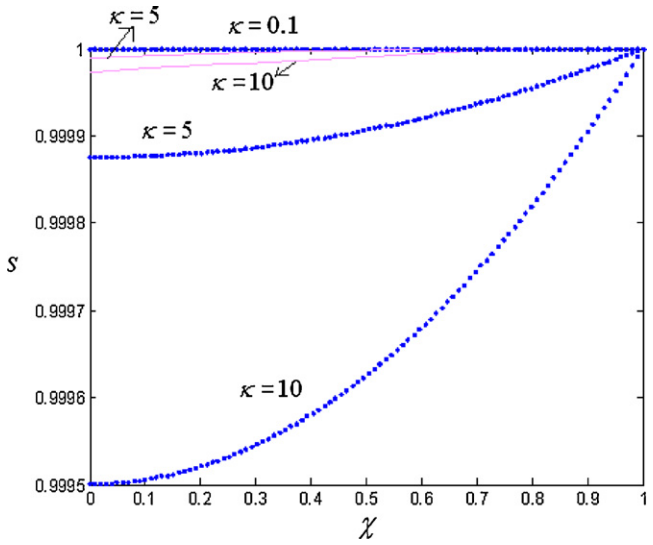

Fig. 6. Plot of the two-dimensional comparative case diagram of the substrate concentration s versus the normalized distance χ when $\gamma a > s/(1+\mu s)$ for $\gamma = 100$, $\eta = 10^5$, $\mu = 0.01$ and $a_\varepsilon = 0.01$ and various values of κ. — is plotted according to Eq. (20), and ··· is plotted according to Eq. (24).

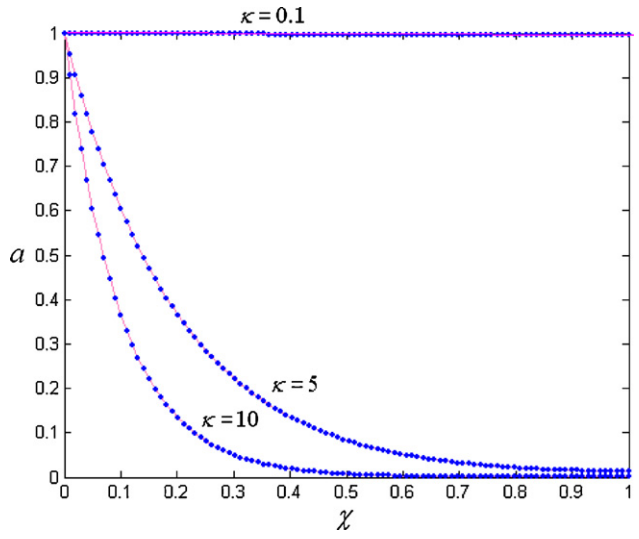

Fig. 8. Plot of the two-dimensional comparative case diagram of the mediator concentration a versus the normalized distance χ for the thin film approximation for $\gamma = 10^{-5}$, $\mu = 0.1$ and $a_\varepsilon = 1$ and various values of κ. — is plotted according to Eq. (19), and ··· is plotted according to Eq. (25).

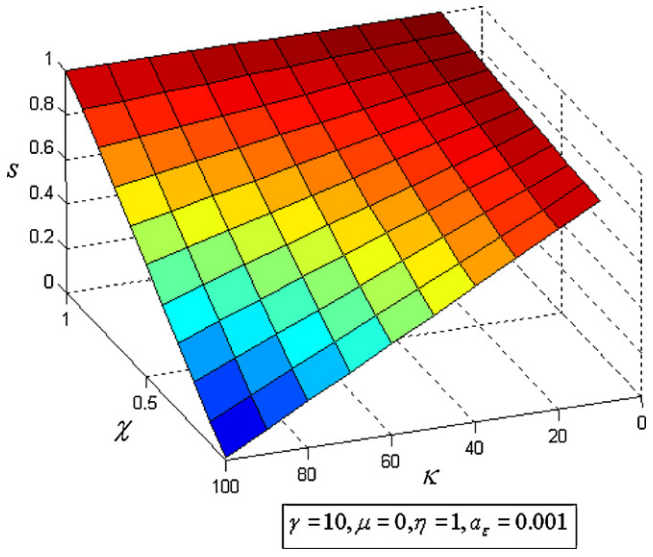

Fig. 7. The normalized three-dimensional substrate concentration profiles s calculated using Eq. (20) for κ in the range of 0–100.

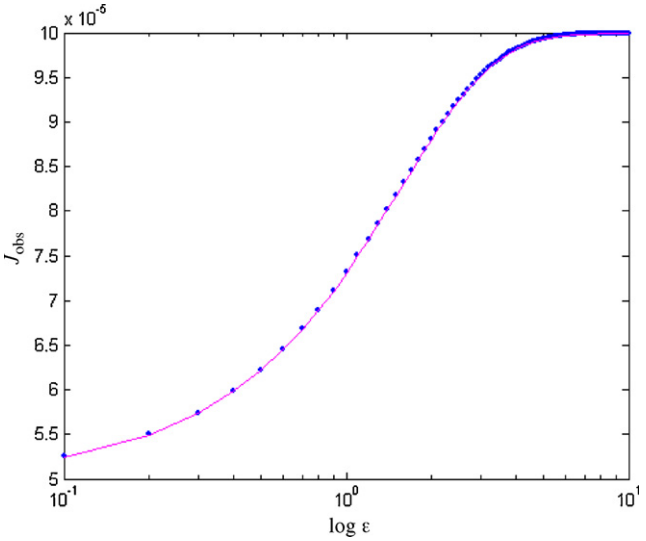

Fig. 9. Comparison of the dimensionless current against ε in the range of 10^{-1} to 10 for $\kappa = 0.01$, $\gamma = 0.001$, $\eta = 0.1$, and $\mu = 0.01$. — is plotted according to Eq. (22), and ··· is plotted according to Eq. (26).

Table 4
Comparison of the mediator concentration a for various values of χ and κ when $\gamma = 0.001$, $\eta = 10$, $\mu = 0.001$ and $a_\varepsilon = 1$.

χ	$\kappa = 0.1$			$\kappa = 5$			$\kappa = 10$		
	This work Eq. (17)	Pratt's work Eq. (23)	% deviation of Eq. (17)	This work Eq. (17)	Pratt's work Eq. (23)	% deviation of Eq. (17)	This work Eq. (17)	Pratt's work Eq. (23)	% deviation of Eq. (17)
0	1	1	0	1	1	0	1	1	0
0.2	0.9982	0.9982	0	0.3680	0.3679	−0.0272	0.1353	0.1353	0
0.4	0.9968	0.9968	0	0.1356	0.1357	−0.0737	0.0183	0.0183	0
0.6	0.9958	0.9958	0	0.0507	0.0507	0	0.0025	0.0025	0
0.8	0.9952	0.9952	0	0.0208	0.0208	0	0.0003	0.0003	0
1	0.9950	0.9950	0	0.0135	0.0135	0	0	0	0
	Average deviation		0	Average deviation		0.0168	Average deviation		0

Table 5
Comparison of the substrate concentration s for various values of χ and κ when $\gamma = 100$, $\eta = 10^5$, $\mu = 0.01$ and $a_\varepsilon = 0.01$.

χ	$\kappa = 0.1$			$\kappa = 5$			$\kappa = 10$		
	This work Eq. (20)	Pratt's work Eq. (24)	% deviation of Eq. (20)	This work Eq. (20)	Pratt's work Eq. (24)	% deviation of Eq. (20)	This work Eq. (20)	Pratt's work Eq. (24)	% deviation of Eq. (20)
0	1	0.9999	0.01	0.9999	0.9998	0.01	0.9999	0.9995	0.04
0.2	1	0.9999	0.01	0.9999	0.9998	0.01	0.9999	0.9995	0.04
0.4	1	0.9999	0.01	0.9999	0.9998	0.01	0.9999	0.9995	0.02
0.6	1	0.9999	0.01	1	0.9999	0.01	0.9999	0.9997	0.02
0.8	1	0.9999	0.01	1	0.9999	0.01	0.9999	0.9998	0
1	1	1	0	1	1	0	1	1	0
	Average deviation		0.008	Average deviation		0.008	Average deviation		0.0266

Table 6
Comparison of the mediator concentration a for the thin film approximation for various values of χ and κ when $\gamma = 10^{-5}$, $\mu = 0.1$ and $a_\varepsilon = 1$.

χ	$\kappa = 0.1$			$\kappa = 5$			$\kappa = 10$		
	This work Eq. (19)	Pratt's work Eq. (25)	% deviation of Eq. (19)	This work Eq. (19)	Pratt's work Eq. (25)	% deviation of Eq. (19)	This work Eq. (19)	Pratt's work Eq. (25)	% deviation of Eq. (19)
0	1	1	0	1	1	0	1	1	0
0.2	0.9982	0.9982	0	0.3680	0.3680	0	0.1353	0.1353	0
0.4	0.9968	0.9968	0	0.1357	0.1357	0	0.0183	0.0183	0
0.6	0.9958	0.9958	0	0.0507	0.0507	0	0.0025	0.0025	0
0.8	0.9952	0.9952	0	0.0208	0.0208	0	0.0003	0.0003	0
1	0.9950	0.9950	0	0.0135	0.0135	0	0	0	0
	Average deviation		0	Average deviation		0	Average deviation		0

3.1.2. *Substrate-limited kinetics ($a/s > 1/\gamma(1+\mu s)$)*

In this case, the enzyme–substrate kinetics is rate limiting. When κ is small, the concentrations of the mediator and the substrate are always close to 1 (Fig. 5). When $\kappa > 1$ and $\chi \geq 0.5$, the concentration of the mediator a reaches the steady-state value. When $\kappa > 1$, the concentration of the substrate increases slowly and reaches the steady-state value 1 (Fig. 6). Fig. 7 shows the three-dimensional concentration profile of the substrate in χ and κ space calculated using Eq. (20). This figure shows that the concentration of the substrate is inversely proportional to κ.

3.1.3. *Thin film approximation*

In this case, $\kappa^2/\eta < 1$ and $s = 1$. The concentration of the mediator is equal to 1 when κ and χ are both less than 1 (Fig. 8). When κ or χ increases, the concentration of the mediator slowly decreases.

Figs. 9–11 show the dimensionless current for various values of κ, γ, η, μ, and a_ε. The current increases as ε increases in the region $-4 < \varepsilon < 2$, and a steady-state appears when $\varepsilon > 2$ and $\varepsilon < -4$ (Fig. 9). The value of the current increases in direct proportion to the values of κ (Fig. 10). The value of the current increases in indirect proportion to the value of μ (Fig. 11).

The mediator concentration a (Eq. (17)) and the substrate concentration s (Eq. (20)) are compared with Pratt's work [6] in Tables 4 and 5. For the thin film approximation, the comparison of the mediator concentration a (Eq. (19)) with Pratt's result [6] is given in Table 6. In all the cases, the average relative error is less than 0.02%.

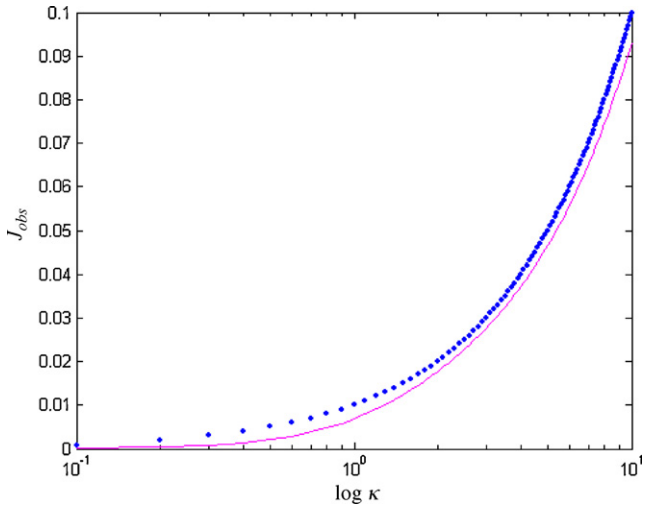

Fig. 10. Comparison of the dimensionless current against κ in the range of 10^{-1} to 10 for $\gamma = 10$, $\eta = 0.01$, $\mu = 0.01$, and $a_\varepsilon = 0.01$. — is plotted according to Eq. (22), and ··· is plotted according to Eq. (27).

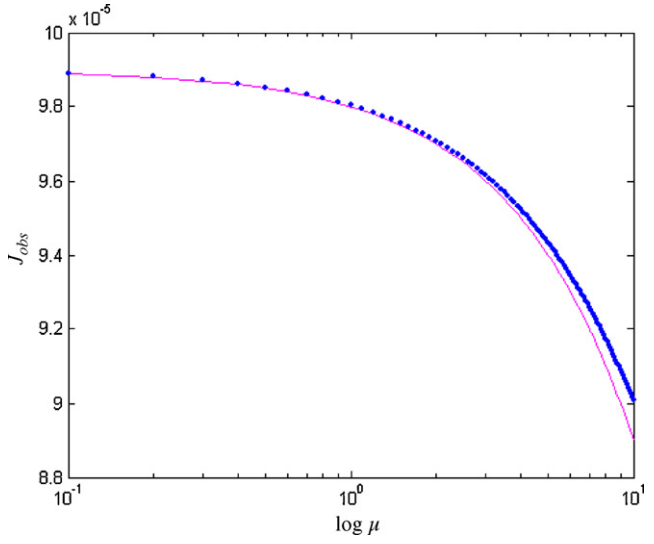

Fig. 11. Comparison of the dimensionless current against μ in the range of 10^{-1} to 10 for $\kappa = 0.01$, $\gamma = 0.01$, $\eta = 0.1$, and $a_\varepsilon = 1$. — is plotted according to Eq. (22), and ··· is plotted according to Eq. (28).

4. Conclusions

A non-linear time-independent differential equation for the polymer-modified electrodes has been formulated and solved using the HPM. The primary result of this work is an approximate calculation of the concentration and current profiles of the mediator and substrate for various values of the parameters κ, γ, η, μ, and a_ε. Our results agree well with the previous limiting case results. This result is very useful for determining the behavior of the system. The extension of the procedure to systems such as the redox hydrogel systems [29,30], in which the mediator and the enzymes are entrapped in a uniform film at the electrode surface, and a study of the effects of mass transport in the bulk solution both seem possible. The analytical result presented here can be used with the approximate analytical formulae to optimize enzyme electrodes. The model may be used to optimize the design of a sensor system by making rational changes to the enzyme loading, film thickness, choice and concentration of the mediator and film properties.

Acknowledgements

It is our pleasure to thank the referees for their valuable comments. This work was supported by the Department of Science and Technology (DST) Government of India. The authors also thank Mr. M.S. Meenakshisundaram, Secretary, The Madura College Board and Dr. T.V. Krishnamoorthy, Principal, The Madura College, Madurai, India, for their constant encouragement.

Appendix A. Basic concepts of the HPM

The HPM method has overcome the limitations of traditional perturbation methods. It can take full advantage of the traditional perturbation techniques, so a considerable deal of research has been conducted to apply the homotopy technique to solve various strong non-linear equations [13,14]. To explain this method, let us consider the following function:

$$D_o(u) - f(r) = 0, \quad r \in \Omega \tag{A1}$$

with the boundary conditions of

$$B_o(u, \frac{\partial u}{\partial n}) = 0, \quad r \in \Gamma \tag{A2}$$

where D_o is a general differential operator, B_o is a boundary operator, $f(r)$ is a known analytical function and Γ is the boundary of the domain Ω. Generally speaking, the operator D_o can be divided into a linear part L and a non-linear part N. Eq. (A1) can therefore be written as:

$$L(u) + N(u) - f(r) = 0 \tag{A3}$$

By the homotopy technique, we construct a homotopy $v(r, p) : \Omega \times [0, 1] \to \Re$ that satisfies:

$$H(v, p) = (1 - p)[L(v) - L(u_0)] + p[D_o(v) - f(r)] = 0 \tag{A4}$$

$$H(v, p) = L(v) - L(u_0) + p\,L(u_0) + p[N(v) - f(r)] = 0. \tag{A5}$$

where $p \in [0,1]$ is an embedding parameter, and u_0 is an initial approximation of Eq. (A1) that satisfies the boundary conditions. From Eqs. (A4) and (A5), we have

$$H(v, 0) = L(v) - L(u_0) = 0 \tag{A6}$$

$$H(v, 1) = D_o(v) - f(r) = 0. \tag{A7}$$

When $p = 0$, Eqs. (A4) and (A5) become linear equations. When $p = 1$, they become non-linear equations. The process of changing p from zero to unity is that of $L(v) - L(u_0) = 0$ to $D_o(v) - f(r) = 0$. We first use the embedding parameter p as a "small parameter" and assume that the solutions of Eqs. (A4) and (A5) can be written as a power series in p:

$$v = v_0 + p\,v_1 + p^2\,v_2 + \ldots \tag{A8}$$

Setting $p = 1$ results in the approximate solution of Eq. (A1):

$$u = \lim_{p \to 1} v = v_0 + v_1 + v_2 + \ldots \tag{A9}$$

This is the basic idea of the HPM.

Appendix B. Approximate analytical solutions of the mediator and substrate

Using the HPM, we construct a homotopy for Eqs. (11) and (12) as follows:

$$(1 - p)\left(\frac{d^2a}{d\chi^2} - \kappa^2\,a\right) + p\left(\frac{d^2a}{d\chi^2} + \gamma\,a\frac{d^2a}{d\chi^2}(1/s + \mu) - \kappa^2\,a\right) = 0 \tag{B1}$$

and

$$(1 - p)\left(\frac{d^2s}{d\chi^2}\right) + p\left(\frac{d^2s}{d\chi^2} + \gamma\,a\frac{d^2s}{d\chi^2}(1/s + \mu) - \gamma\,\eta^{-1}\,\kappa^2\,a\right) = 0 \tag{B2}$$

The approximate solution of (B1) is

$$a = a_0 + p\,a_1 + p^2 a_2 + \ldots \tag{B3}$$

and the approximate solution of (B2) is

$$s = s_0 + p\,s_1 + p^2\,s_2 + \ldots \tag{B4}$$

Substituting Eq. (B3) into Eq. (B1) and arranging the coefficients of p powers, we have

$$p^0 : \frac{d^2a_0}{d\chi^2} - \kappa^2\,a_0 = 0 \tag{B5}$$

$$p^1 : \frac{d^2a_1}{d\chi^2} - \kappa^2\,a_1 + \gamma\,a_0\frac{d^2a_0}{d\chi^2}\left(\frac{1}{s_0} + \mu\right) = 0 \tag{B6}$$

$$p^2 : \frac{d^2a_2}{d\chi^2} - \kappa^2\,a_2 + \gamma\,a_1\frac{d^2a_0}{d\chi^2}\left(\frac{1}{s_0} + \mu\right) + \gamma\,a_0\frac{d^2a_1}{d\chi^2}\left(\frac{1}{s_0} + \mu\right) - \gamma\frac{d^2a_0}{d\chi^2}a_0\frac{s_1}{s_0^2} = 0 \tag{B7}$$

Substituting Eq. (B4) into Eq. (B2) and arranging the coefficients of p powers, we have

$$p^0 : \frac{d^2s_0}{d\chi^2} = 0 \tag{B8}$$

$$p^1 : \frac{d^2s_1}{d\chi^2} - \gamma\,\eta^{-1}\,\kappa^2\,a_0 + \gamma\,a_0\frac{d^2s_0}{d\chi^2}\left(\frac{1}{s_0} + \mu\right) = 0 \tag{B9}$$

$$p^2 : \frac{d^2s_2}{d\chi^2} - \gamma\,\eta^{-1}\,\kappa^2\,a_1 + \gamma\,a_0\frac{d^2s_1}{d\chi^2}\left(\frac{1}{s_0} + \mu\right) + \gamma\,a_1\frac{d^2s_0}{d\chi^2}\left(\frac{1}{s_0} + \mu\right) - \gamma a_0\frac{d^2s_0}{d\chi^2}\frac{s_1}{s_0^2} = 0 \tag{B10}$$

The initial approximations are as follows:

$$a_0(0) = a_\varepsilon, \qquad a_0'(1) = 0, \qquad a_i'(1) = 0 \quad \text{for all } i = 1, 2, 3, \ldots \tag{B11}$$

$$s_0(1) = 1, \qquad s_0'(0) = 0, \qquad s_i'(0) = 0, \quad \text{for all } i = 1, 2, 3, \ldots \tag{B12}$$

From Eq. (B5) we get

$$a_0 = W_2 \cosh(\kappa(1-\chi)). \tag{B13}$$

From Eq. (B8) we get

$$s_0 = 1. \tag{B14}$$

Substituting Eq. (B13) and Eq. (B14) into Eq. (B6), we obtain the solution to Eq. (B6):

$$a_1 = W_1 [\cosh \kappa(\cosh(2\kappa(1-\chi)) - 3) + (3 - \cosh 2\kappa)\cosh(\kappa(1-\chi))]. \tag{B15}$$

Using Eqs. (B13)–(B15) in Eq. (B9) and then solving we get

$$s_1 = \frac{\gamma W_2}{\eta} [-(1 + \kappa \sinh \kappa) + (\kappa \sinh \kappa)\chi + \cosh(\kappa(1-\chi))]. \tag{B16}$$

Using Eqs. (B13)–(B16) and Eq. (B7) we get

$$a_2 = W_3(W_4 + W_5 + W_6)(-2\chi + \chi^2). \tag{B17}$$

Using Eq. (B13)–(B16) in Eq. (B10) and then solving Eq. (B10) we obtain:

$$s_2 = \frac{\gamma W_1}{2\eta} [2(\cosh 2\kappa - 3)[1 + (\kappa \sinh \kappa)(1-\chi) - \cosh(\kappa(1-\chi))] + \cosh \kappa[1 + (1-\chi)(2\kappa \sinh 2\kappa - 6\kappa^2(\chi+1)) - \cosh(2\kappa(1-\chi))]] \tag{B18}$$

Adding Eqs. (B13), (B15) and (B17), we get Eq. (17) (the concentration of the mediator, a) in the text. Similarly, by adding Eqs. (B14), (B16) and (B18) we get Eq. (20) (the concentration of the substrate, s) in the text.

References

[1] R. Baronas, F. Ivanauskas, J. Kulys, Mathematical Modeling of Biosensors Springer Series on Chemical Sensors and Biosensors, vol 9, 2010.
[2] R. Baronas, F. Ivanauskas, J. Kulys, Sensors 6 (2006) 453.
[3] M. Kosiborod, S.S. Rathore, S.E. Inzucchi, et al., J. Theor. Comput. Chem. 7 (2008) 113.
[4] C.K. Naber, R.H. Mehta, C. Jünger, et al., J. Electroanal. Chem. 131 (1982) 1.
[5] K.K. Lee, S.P. Fortmann, J.M. Fair, et al., J. Electroanal. Chem. 170 (1984) 27.
[6] P.N. Bartlett, K.F.E. Pratt, J. Electroanal. Chem. 397 (1995) 61.
[7] W.J. Blaedel, T.R. Kissel, R.C. Boguslavski, Anal. Chem. 44 (1972) 2030.
[8] J.J. Kulys, V.V. Sorochinslii, R.A. Vidziunaite, Biosensors 2 (1986) 135.
[9] P.N. Bartlett, R.G. Whitaker, J. Electronal. Chem. 224 (1987) 27.
[10] F.A. Masoudi, M.E. Plomondon, D.J. Magid, A. Sales, J.S. Rumsfeld, Biosens. Bioelectron. 8 (1993) 451.
[11] V. Flexer, K.F.E. Pratt, F. Garay, P.N. Bartlett, E.J. Calvo, J. Electroanal. Chem. 616 (2008) 87.
[12] R. Senthamarai, L. Rajendran, Electrochim. Acta 55 (2010) 3223.
[13] X.C. Cai, W.Y. Wu, M.S. Li, Int. J. Nonlinear. Sci. Numer. Simulat. 7 (1) (2006) 109.
[14] P.D. Ariel, Nonlinear. Sci. Lett. A. 1 (2010) 43.
[15] Q.K. Ghori, M. Ahmed, A.M. Siddiqui, Int. J. Nonlinear Sci. Numer. Simulat. 8 (2) (2007) 179.
[16] T. Ozis, A. Yildirim, Int. J. Nonlinear Sci. Numer. Simulat. 8 (2) (2007) 243.
[17] S.J. Li, Y.X. Liu, Int. J. Nonlinear Sci. Numer. Simulat. 7 (2) (2006) 177.
[18] M.M. Mousa, S.F. Ragab, Z. Naturforsch. 63 (2008) 140.
[19] J.H. He, Comput. Method Appl. Mech. Eng. 178 (1999) 257.
[20] J.H. He, Appl. Math. Comput. 135 (2003) 73.
[21] J.H. He, Appl. Math. Comput. 140 (2003) 217.
[22] J.H. He, Phys. Lett. A 350 (2006) 87.
[23] A. Golbabai, B. Keramati, Chaos Soliton Fractals 37 (2008) 1528.
[24] M. Ghasemi, M. Tavassoli Kajani, E. Babolian, Appl. Math. Comput. 188 (2007) 446.
[25] J. Biazar, H. Ghazvini, Chaos Soliton Fractals 39 (2009) 770.
[26] Z. Odibat, S. Momani, Phys. Lett. A 365 (2007) 351.
[27] M.S.H. Chowdhury, I. Hashim, Phys. Lett. A 368 (2007) 305.
[28] J.H. He, Int. J. Modern Phys. B 20 (10) (2006) 1141.
[29] B.A.H.A. Gregg, Anal. Chem. 62 (1990) 258.
[30] I. Tomatssu, A. Hashidzume, A. Harada, Macromol. Rapid Commun. 27 (2006) 238.